Boltorn-Modified Poly(2,6-dimethyl-1,4-phenylene oxide) Gas Separation Membranes

Dana M. Sterescu,[†] Dimitrios F. Stamatialis,*[,†] Eduardo Mendes,[‡] Jan Kruse,[§] Klaus Rätzke,[§] Franz Faupel,[§] and Matthias Wessling[†]

University of Twente, Faculty of Science and Technology, Membrane Technology Group, PO. Box 217, 7500 AE, Enschede, The Netherlands, Delft University of Technology, Polymer Materials and Engineering, 2628 BL, Delft, The Netherlands, and Lehrstuhl für Materialverbunde, Technische Fakultät der Christian-Albrechts-Universität zu Kiel, Kaiserstrasse 2, 24143 Kiel, Germany

Received April 1, 2007; Revised Manuscript Received May 24, 2007

ABSTRACT: This paper describes the preparation, characterization and the permeation properties of poly(2,6-dimethyl-1,4-phenylene oxide) (PPO) dense polymer films containing aliphatic hyperbranched polyesters, Boltorn (H20, H30, and H40). The Boltorn are dispersed in PPO at various concentrations. The gas permeability results were very different between low and high concentration of Boltorn. The gas permeability of PPO with 1.0 wt % of Boltorn is 2−3 times higher than the pure polymer, while at higher concentration (9.1 wt %) of Boltorn the permeability becomes almost 50% of the pure polymer. The gas pair selectivity, however, stays constant. The increase in permeability at low concentration of Boltorn is due to the increase of the free volume, probably due to hydrogen bonds between Boltorn and the oxygen of PPO backbone. The decreased permeability of PPO containing higher concentration of Boltorn (9.1 wt %) is due to two reasons: decrease in free volume as determined by PALS as well as phase separation. The hyperbranced polyesters form aggregates that migrate to the top surface of the membrane.

1. Introduction

The control of gas permeability and selectivity for polymer membranes separating gases is a subject of intense research in both industry and academia,[1] focusing on the relationship between the polymer structure and gas separation properties. Most of the polymers that have been investigated, however, show the general trend that highly permeable polymers possess rather low selectivity and vice versa (permeability/selectivity trade off relationship[2]).

The permeation properties of a polymer depend primarily on the packing density, the polymer chain mobility and the free volume of the polymer. Poly(2,6-dimethyl-1,4-phenylene oxide) (PPO) is one of the very few polymers that are actually used for the industrial production of gas separation membranes.[3] Because of its high permeability and acceptable selectivity, PPO is particularly interesting for the production of nitrogen-enriched air. It is desirable to increase permeability of PPO without compromising selectivity. For this, a considerable interest has been shown in dendritic polymers. The materials are called hyperbranched polymers (HBP), to distinguish them from monodisperse dendrimers. Unique features of the dendritic architecture[4−6] result directly from the repetitive branching which occurs during their synthesis giving access to large number of reactive end groups. Because of their availability of free volume,[7] they might be attractive to control permselectivities for small molecules like gases for gas separation applications.

In fact, this paper presents a successful increase of gas permeability based on commercially available aliphatic hyperbranched polyesters, Boltorn, mixed with PPO matrix. Small amount of Boltorn dispersed into PPO causes significant increase of membrane permeability, while at higher amounts the gas permeability decreases. A systematic analysis of PPO−Boltorn membranes is performed using scanning electron microscopy (SEM), differential scanning calorimetry (DSC), Wide-angle X-ray scattering (WAXS), positron annihilation lifetime spectroscopy (PALS), energy dispersive X-ray analysis (EDX) measurements, and gas sorption experiments in order to investigate the influence of Boltorn concentration to the membrane permeation performance. It seems that at low Boltorn concentration, the high gas permeability in comparison to pure PPO is due to increase polymer free volume by the Boltorn. At higher Boltorn concentration, the free volume decreases and the Boltorn form clusters. Both phenomena cause decrease of gas permeability.

2. Experimental Section

2.1. Materials. For the membrane preparation the following materials were used: Poly(2,6-dimethyl-1,4-phenylene oxide) (PPO) (Parker Filtration and Separation, MW = 150000 measured by GPC), chloroform (Merck), 1-methyl-2-pyrrolidinone (NMP, 99%, Acros Organics), and hyperbranched polymers commercially available as Boltorn H20, H30, and H40 (kindly supplied by Perstorp Specialty Chemicals AB, Sweden).

The hyperbranched polymers studied in this work are aliphatic polyesters using ethoxylated pentaerythritol as central cores and 2,2-bis(methylol)propionic acid (bis-MPA) as dendritic units. Boltorn H20 statistically contains two generations of bis-MPA, while Boltorn H30 and H40 have three and four generations of MPA, respectively. An example of Boltorn is shown in Figure 1. The products are all hydroxyl functional, but differ in molecular weight ($M_{w,H20}$ = 2100 g/mol, $M_{w,H30}$ = 3500 g/mol, $M_{w,H40}$ = 5100 g/mol) and hydroxyl functionality. Hydroxyl number, molecular weight and polydispersity of the Boltorn polymers from the data sheet provided by Perstorp are presented elsewhere.[5,8]

2.2. Preparation of PPO and PPO—Boltorn Membranes. For the preparation of pure PPO membranes, the PPO was dissolved

* Corresponding author. E-mail: d.stamatialis@tnw.utwente.nl. Telephone: +31 53 4894675. Fax: +31 53 4894611

[†] Membrane Technology Group, Faculty of Science and Technology, University of Twente.

[‡] Polymer Materials and Engineering, Delft University of Technology.

[§] Lehrstuhl für Materialverbunde, Technische Fakultät der Christian-Albrechts-Universität zu Kiel.

10.1021/ma070772g CCC: $37.00
Published on Web 06/27/2007

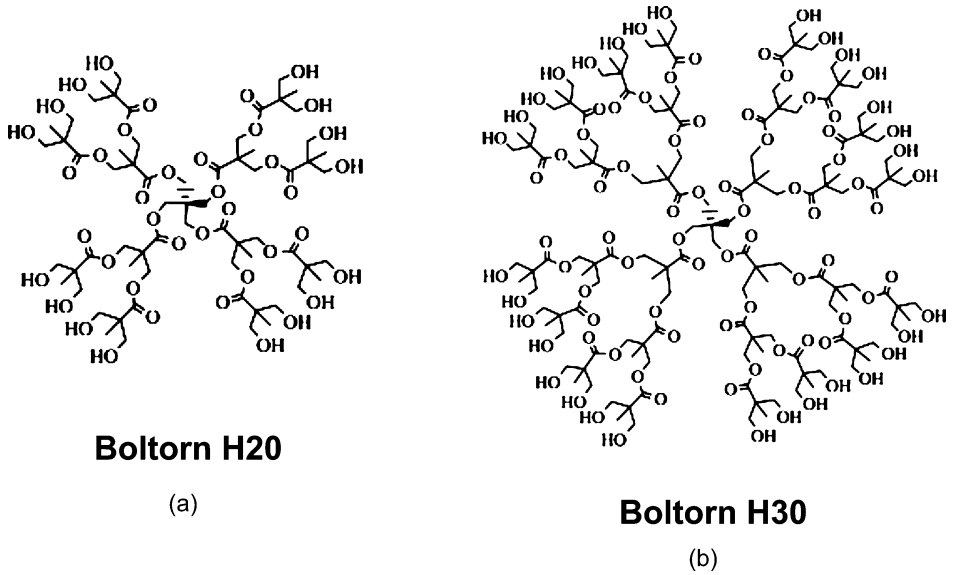

Figure 1. Schematic representation of the hyperbranched polyol molecule (a) Boltorn H20 and (b) Boltorn H30 structure.

in chloroform (10 wt % polymer solution). The solution was cast on a glass plate and dried first under nitrogen atmosphere at room temperature (20−25 °C) for 3 days and then in a vacuum oven at 50 °C under nitrogen atmosphere for 2 days. Films of 40−70 μm thickness were prepared.

For the preparation of PPO membranes dispersed with Boltorn (three different generations: H20, H30, and H40), the PPO and Boltorn were dissolved separately: PPO in chloroform (10 wt % polymer solution) and the Boltorn in NMP (10 wt % Boltorn solution), respectively. Both solutions were stirred at room temperature until complete dissolution (for 3−4 h). Then, the two solutions were mixed and stirred for 4 h until they became homogeneous. The PPO-dispersed Boltorn solutions were cast on a glass plate and dried under nitrogen atmosphere at room temperature (20−25 °C) for 3 days. Then, the PPO−Boltorn films of 40−70 μm thickness were peeled off from the glass plate and dried in a vacuum oven at 30 °C until constant weight (for approximately 2 months). Films containing 0.5, 1.0, 2.4, 4.8, 7.0, and 9.1 wt % of Boltorn/membrane were prepared. The preparation of mechanically stable films containing more than 9.1 wt % of Boltorn was not possible. The amount of Boltorn in the membrane was calculated using the equation:

$$\text{wt \% (Boltorn/membrane)} = \frac{g_{\text{Boltorn}}}{g_{\text{Boltorn}} + g_{\text{PPO}}} \times 100 \qquad (1)$$

For comparison, pure PPO membranes were also prepared by dissolution of the polymer in mixture of $CHCl_3$/NMP, following the procedure for the preparation of PPO−Boltorn membranes. In this case, however, this was done without the addition of Boltorn.

2.3. Characterization of Membranes.

DSC Measurements. The thermal properties of pure PPO and PPO−Boltorn dispersed were measured using a Perkin-Elmer DSC-7 (differential scanning calorimeter) in nitrogen atmosphere. The PPO−Boltorn samples were initially heated from −60 until +350 °C, cooled with liquid nitrogen, held for 5 min, and reheated two more times following the same steps, under nitrogen atmosphere. The heating rate was 10 °C/min, and the cooling rate was 20 °C/min. The glass transition temperature, T_g, of the polymer was obtained from the third scan.

Gas Permeability and Sorption. The permeation of pure nitrogen (N_2), oxygen (O_2), and carbon dioxide (CO_2) through the PPO and PPO−Boltorn membranes was investigated at different feed pressures (1.5, 2.5, and 3.5 bar), using the set up described elsewhere.[9] Pure gas permeability coefficients were calculated from the steady-state pressure increase in time in a calibrated volume at the permeate side by using the equation:

$$\frac{\text{P}}{l} = \frac{\text{V}\cdot 273.15\cdot(P_{\text{pt}} - P_{\text{p0}})}{\text{A}\cdot\text{T}\cdot\dfrac{(P_{\text{ft}} + P_{\text{f0}})}{2}\,76t} \times 10^6 \qquad (2)$$

where the ideal gas law is assumed to be valid, P_{pt}, P_{ft} [bar] is the pressure at the permeate and feed side at time t, P_{p0} and P_{f0} are the permeate and feed pressure at $t = 0$, T [K] is the temperature, V [cm^3] is the calibrated permeate volume, and A [cm^2] is the membrane area. The gas permeance (P/l) is expressed in GPU, i.e., 10^{-6} cm^3 cm^{-2} s^{-1} $cmHg^{-1}$. Multiplying the gas permeance with the thickness of dense membrane, l [cm], gives the permeability coefficient in Barrer. All the gas permeation experiments were performed at 35 °C. Values and error bars reported in the tables and figures are based on measurements of two different membrane samples.

The gas sorption isotherms of N_2, O_2, and CO_2 in dense PPO pure (in $CHCl_3$), PPO pure (in $CHCl_3$/NMP), and PPO−Boltorn dispersed (1.0 and 9.1 wt %) films were measured at 35 °C, using a magnetic suspension balance[10] (MSB, Rubotherm). The experimental procedure was divided into five steps: (a) evacuation of pressure vessel and sample for at least 24 h; (b) increase of gas pressure to desired value; (c) wait until equilibrium in mass change is reached; (d) record equilibrium mass, temperature, and pressure; (e) repeat steps b and c or if the maximum pressure is reached: evacuate sample (step a) and start measurement with new gas or new sample. The equilibrium mass increase was corrected for buoyancy by subtracting the weight at zero sorption at a certain pressure from the vacuum weight of the sample. Using the equilibrium weight increase and the density of the polymer, the concentration (in cm^3 STP) inside the polymer (cm^3 polymer) was calculated.[10]

Crank[11] showed that the sorption of a penetrant in a polymer matrix is proportional to the square root of time, assuming a constant diffusion coefficient. This behavior is called ideal Fickian sorption and the mass uptake (g) in time (M(t)) can be described with the following equation:

$$\frac{M(t)}{M_\infty} = 1 - \frac{8}{\pi^2}\sum_{m=0}^{\infty}\frac{1}{(2m+1)^2}\exp\left\{-\frac{D(2m+1)^2\pi^2 t}{l^2}\right\} \qquad (3)$$

where M_∞ is the amount of mass (g) sorbed by Fickian sorption at infinite time, D is the diffusion coefficient (m^2/s), t is the time (s),

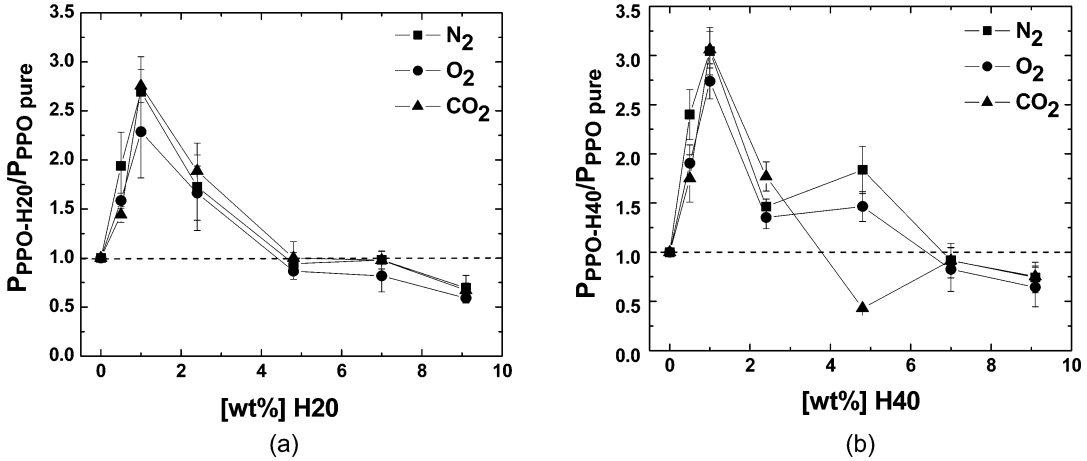

Figure 2. Permeability of (a) PPO−H20 and (b) PPO−H40 normalized with the permeability of pure PPO (in $CHCl_3$) vs the wt % Boltorn content for gases N_2 (■), O_2 (●), and CO_2 (▲) at 1.5 bar feed pressure and 35 °C.

and l is the sample thickness (m). Fitting of the sorption data into this equation leads to the diffusion coefficients.[12]

Scanning Electron Microscopy (SEM). The geometrical characteristics and the morphology of the membranes were determined using a Jeol JSM-5600 LV Scanning Electron microscope. The membrane samples were cut and sputtered with a thin layer of gold using a Balzers Union SCD 040 sputtering apparatus.

Energy Dispersive X-ray Analysis (EDX). The local elemental composition of the PPO−Boltorn membranes was investigated by energy dispersive X-ray analysis (EDX) using a NORAN System Six (NSS) microanalysis system model C100 (Thermo Electron Corporation). This technique is used in conjunction with SEM type JSM-6480LV.

WAXS Measurements. Wide-angle X-ray scattering (WAXS) experiments were performed using a Bruker-Nonius D8-Discover equipped with 2D detector. Standard background (air and sample holder) subtraction measured at the same time and conditions were applied to all data. The sample−detector (S−D) distance was set at 10 cm and the incident beam wavelength was 1.54 Å (Cu Kα). Measurements were performed both in a perpendicular manner and in the plane of the membrane.[13] In the first case, the sample thickness as seen by the incident beam was always less than 0.5 mm.

Positron Annihilation Lifetime Spectroscopy (PALS). A well accepted method to determine free volume in polymers[14] is positron annihilation lifetime spectroscopy (PALS). Positrons obtained from radioactive decay annihilate with electrons in the polymer material probing the local electron density and hence atomic density. Once injected from a radioactive source, positrons form in most polymers hydrogen-like positronium (Ps) states. The pick-off lifetime of orthopositronium, (τ_{o-Ps}), is well correlated to the free-volume hole size in polymers. If the spins of electron and positron add to value of one, annihilation of orthopositronium (o-Ps) is obstructed, reducing the decay rate drastically.[15] The annihilation is due to the interaction of the o-Ps with the electrons in the surrounding material because an exchange of the electrons can change the state of the orthopositronium into the fast decaying para-state. Thus, the local electron density, which is lower in larger holes, becomes a measure for the hole size. The success of PALS in polymer research is largely due to the so-called standard model developed by Tao and Eldrup.[16,17] This simple quantum mechanical model assumes the Ps to be confined to spherical holes with infinitely high walls and gives direct relationship between τ_{o-Ps} and the size of free volume holes. Since hole sizes in amorphous polymers are relatively broadly distributed, the discrete τ_{o-Ps} obtained from the fit to lifetime spectra and hence the hole radius has to be regarded as an average value.[18] On the other hand, the interpretation of the o-Ps intensity, which has often been used as a measure for the hole concentration, is questionable, as the intensity is also affected by the positronium formation probability.[19] Therefore, it will not be considered in the present paper. The average decay rate of orthopositronium in our membranes was measured and was correlated to the polymer free volume.

Positron annihilation experiments have been performed in a fast−fast coincidence setup with a home made temperature-controllable sample holder under high vacuum conditions.[15] Polymeric thin films were cut into 9×9 mm^2 pieces and stacked together with a Na-22 source (1MBq) in a sandwich like manner (total thickness ≈ 0.8 mm each) to ensure complete absorption of the positrons in the sample. The sandwich was wrapped into aluminum foil and put into a sample holder. Spectra were recorded with 10^7 counts within 12 h, typically. Evaluation was performed with the LT9.0 routine program using the common background subtraction and the final resolution function, which was determined as a sum of two Gaussians with FWHMs (full width at half-maximum) of approximately 247 and 390 ps and weight of 80% and 20%; three lifetime components were assumed, where the first was kept fixed at 125 ps (lifetime of p-Ps in vacuum).

3. Results and Discussion

3.1. Gas Permeability. Figure 2 shows the gas permeability of PPO−H20 and PPO−H40 in comparison to pure PPO (prepared in $CHCl_3$) membranes. The permeability coefficient reaches a maximum value at 1.0 wt % and decreases with further increase of Boltorn concentration up to 9.1 wt %, where it becomes lower than PPO pure. Similar trend was found for all three gases measured, N_2, O_2, and CO_2 and for the three generations of Boltorn (H20, H30, and H40) (see Figure 3). Besides, the gas permeability through pure PPO membranes and PPO−Boltorn is constant at different feed pressures for all three gases measured (see Figure 4 an example for O_2).

According to the literature,[20] it is common that the casting solvent has an influence on membrane properties. To find the reason for the significant increase of gas permeability (Boltorn or/and of the casting solvent) we also compared the PPO−Boltorn membranes to pure PPO prepared in the same $CHCl_3$/NMP solvent mixture (see membrane preparation). Table 1 shows the gas permeability of PPO pure (in $CHCl_3$), PPO−H40 1.0 wt %, PPO−H40 9.1 wt % and the pure PPO membranes prepared in the same $CHCl_3$/NMP solvent mixture. The results show indeed a difference in gas permeability between pure PPO prepared in various solvents. The nitrogen permeability coefficient of PPO−H40 1.0 wt % increases 89% in comparison to PPO pure in the same $CHCl_3$/NMP mixture and 207% in comparison to PPO pure (in $CHCl_3$). Similar behavior was found also for O_2 and CO_2 gases. For PPO−H40 9.1 wt %, the nitrogen permeability coefficient decreases 43%

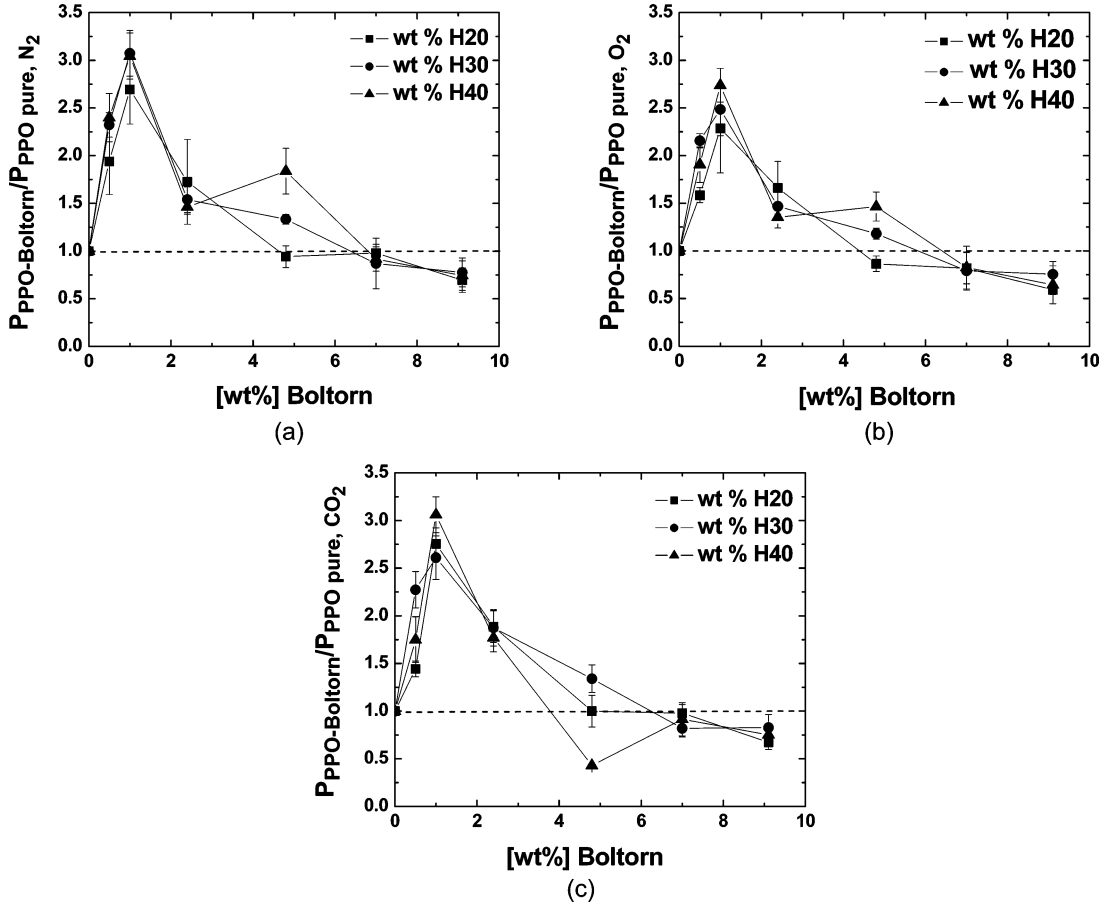

Figure 3. Permeability of PPO−Boltorn (H20(■), H30 (●), and H40(▲)) normalized with the permeability of pure PPO (in $CHCl_3$) vs the wt % Boltorn content for gases (a) N_2, (b) O_2, and (c) CO_2 at 1.5 bar feed pressure and 35 °C.

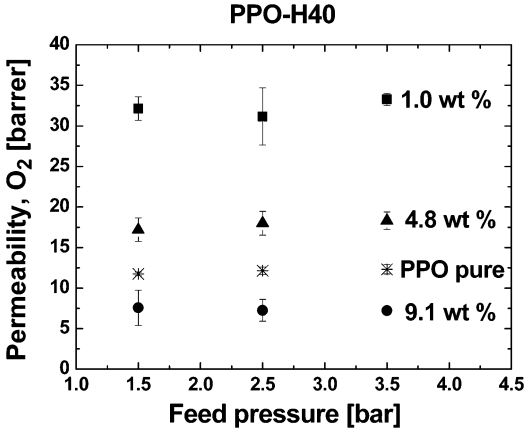

Figure 4. Oxygen permeability of PPO−H40 vs feed pressure at various H40 concentrations: 1.0 wt % (■), 4.8 wt % (▲), 9.1 wt % (●), and pure PPO (in $CHCl_3$) (∗) at 35 °C.

Table 1. Permeability Results of PPO and PPO−H40 Films (Feed Pressure: 1.5 Bar, T = 35 °C)

	permeability of gases [barrer]		
membranes	N_2	O_2	CO_2
PPO pure ($CHCl_3$)	2.7 ± 0.1	11.7 ± 0.2	50.7 ± 2.6
PPO pure ($CHCl_3$/NMP)	4.4 ± 0.2	16.2 ± 0.5	63.9 ± 1.6
PPO−H40 1.0 wt % H40	8.3 ± 0.6	32.1 ± 1.5	155.1 ± 1.4
PPO pure ($CHCl_3$/NMP)	3.5 ± 0.1	16.1 ± 0.3	65.7 ± 1.2
PPO−H40 9.1 wt % H40	2.0 ± 0.4	7.6 ± 2.2	38.1 ± 3.5

in comparison to PPO pure prepared in the same $CHCl_3$/NMP mixture, instead of 26% in comparison to PPO pure (in $CHCl_3$). These results demonstrate that both the Boltorn and the casting solvent have an influence on the gas membrane permeability.

Table 2. Ideal Gas Selectivities of PPO and PPO−H40 Films (Feed Pressure, 1.5 Bar; T = 35 °C)

	selectivity		
membranes	P_{O_2}/P_{N_2}	P_{CO_2}/P_{N_2}	P_{CO_2}/P_{O_2}
PPO pure ($CHCl_3$)	4.3 ± 0.1	18.7 ± 1.1	4.3 ± 0.3
PPO−H40 0.5 wt %	3.4 ± 0.6	13.6 ± 2.5	4.0 ± 0.7
PPO−H40 1.0 wt %	3.9 ± 0.5	18.8 ± 1.5	4.8 ± 0.3
PPO−H40 2.4 wt %	4.0 ± 0.4	22.6 ± 1.7	5.6 ± 0.5
PPO−H40 4.8 wt %	3.5 ± 0.7	14.5 ± 1.9	4.2 ± 0.4
PPO−H40 7.0 wt %	3.9 ± 1.5	18.6 ± 5.1	4.8 ± 1.9
PPO−H40 9.1 wt %	3.8 ± 1.8	18.9 ± 5.5	5.0 ± 1.9

Table 2 presents the ideal gas selectivity of PPO−H40 and pure PPO (in $CHCl_3$) at a feed pressure of 1.5 bar corresponding to the average of two different membrane samples. Similar results were found also for pure PPO (in $CHCl_3$/NMP). The selectivity generally stays constant (if one takes into account the standard deviation). Some exceptions are observed for the films with 0.5, and 4.8 wt % Boltorn. Their CO_2/N_2 selectivity decreases approximately 22−27% than the pure PPO, while it increases for PPO−Boltorn 2.4 wt %. Similar values of the ideal gas selectivity were found also for PPO−H20 and PPO−H30 membranes.

3.2. Scanning Electron Microscopy (SEM). Scanning electron microscopy (SEM) was used to investigate the distribution of Boltorn in the PPO structure. Figure 5 shows some typical results for our membranes. The micrographs were obtained using a Jeol JSM-5600 LV scanning electron microscope with magnifications of 950× and 5000×.

The SEM micrographs of pure PPO (in $CHCl_3$) and pure PPO (in $CHCl_3$/NMP) show similar dense and compact structure (see Figure 5a). At higher Boltorn concentration in PPO however,

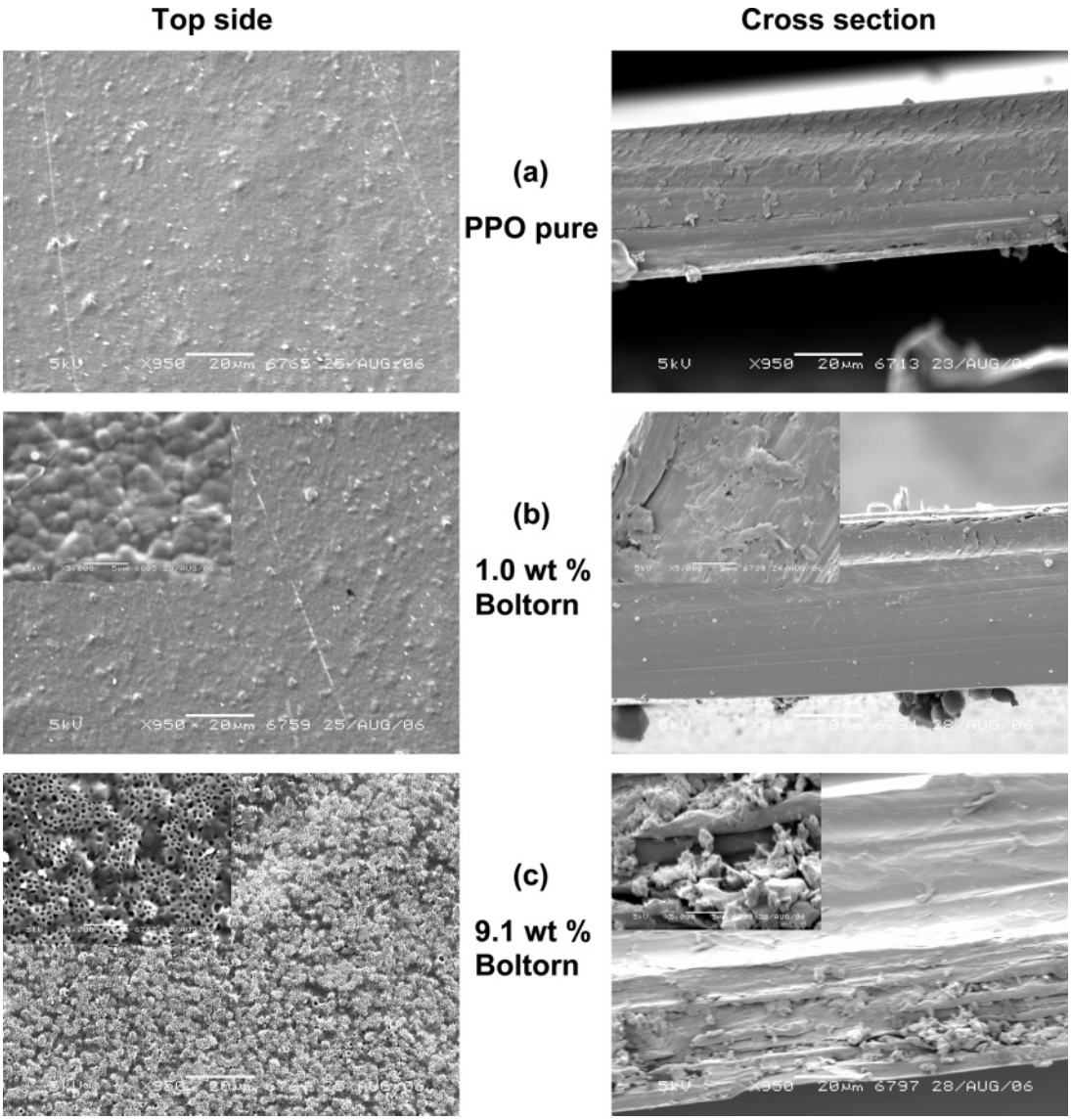

Figure 5. SEM micrographs of PPO and PPO−H40 membranes containing various Boltorn H40 concentrations (insets are zoom at magnification 5000x).

phase separation occurs resulting in a dispersed particulate structure (see Figure 5), in agreement with Boogh et al.[21] The PPO−H40 1.0 wt % membrane (Figure 5b) has a dense and compact structure comparable with the pure polymer. The formation of the particulate structure is mostly visible at higher Boltorn concentration (Figure 5c). The PPO−H40 9.1 wt % membrane seems to be different at each side, one dense homogeneous layer at the glass side and one more heterogeneous layer at the air side (Figure 5c).

The absence of phase separation at low concentration of H40 (1.0 wt %) in PPO is probably due to the network formation linking the hyperbranched molecules to PPO chain by the hydrogen bonds.[21] An indication of this is given by the unchanged surface structure after washing of the membrane with NMP solvent. For this, we kept the PPO−Boltorn membranes 4 days in NMP (known as good solvent for Boltorn, but not for PPO). The membranes were dried afterwords in N_2 box for 2 days and vacuum oven at 80 °C for 2 days and analyzed again by SEM. The SEM micrographs of PPO−H40 1.0 wt % after "washing" with NMP look similar to the pure PPO suggesting that no Boltorn was washed out from the membrane surfaces. In contrary, PPO−H40 9.1 wt % washed in NMP has "holes" at the top surface, instead of the dispersed particulate structure seen before (see Figure 6). The "holes" were probably created after dissolution of Boltorn by NMP, while the glass side keeps its dense structure similar to the pure PPO. This test suggests that at low Boltorn concentrations (1.0 wt %), Boltorn is well mixed into the polymer structure, while for higher concentrations (9.1 wt %) the Boltorn migrates to the air surface and forms agglomerates. Because of the formation of such composite structure higher concentrations of Boltorn lead to loss in mechanical strength. Therefore, mechanically stable membranes containing higher concentrations of Boltorn than 9.1 wt % could not be prepared.

3.3. Energy Dispersive X-ray Analysis (EDX). The surface compositions of 6 different samples were analyzed by EDX. The carbon (C) and oxygen (O) content of the pure Boltorn (H40), pure PPO (in $CHCl_3$), pure PPO (in $CHCl_3$/NMP), and PPO−H40 samples were measured. The results of pure PPO (in $CHCl_3$) and pure PPO (in $CHCl_3$/NMP) are similar; therefore, we compared the PPO−H40 to pure PPO (in $CHCl_3$) (see Table 3). The average C/O ratio of pure PPO is 8/1 instead of 5/3 for pure Boltorn (H40). The PPO−H40 1 wt % and PPO-pure membrane show almost the same C and O content, whereas the PPO−H40 9.1 wt % shows slightly lower carbon content at air side surface than the PPO-pure sample. This difference is

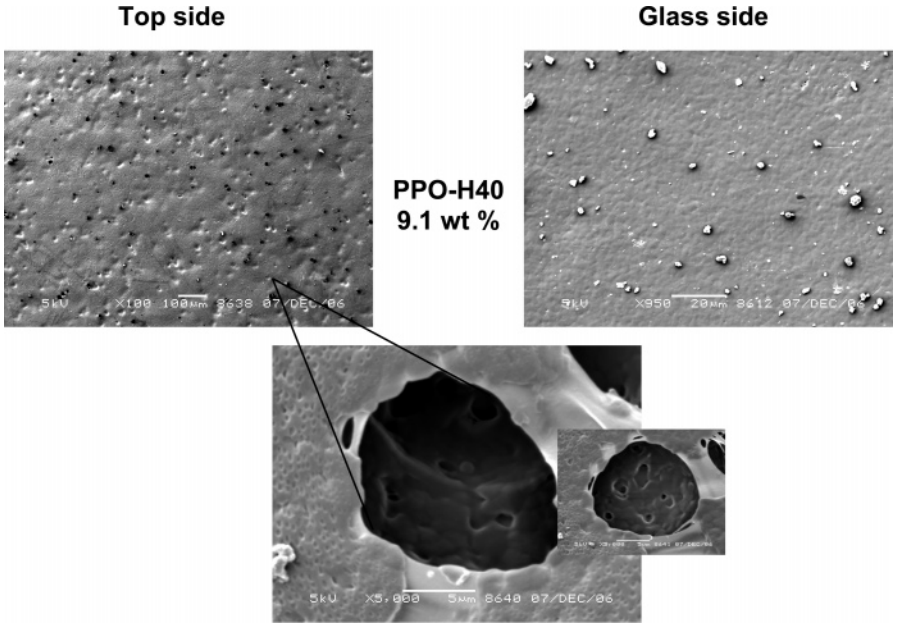

Figure 6. SEM micrographs of PPO−H40 9.1 wt % (that includes a zoom of the top surface, 5000x).

small, because the average composition of the surface is compared. If the carbon content is measured locally the differences become more significant. Figure 7 shows the EDX-SEM micrograph and the corresponding carbon content of the PPO−H40 9.1 wt % vs the position at the membrane surface. The agglomerates visible on the PPO−H40 air side contain significantly lower amount of carbon than the rest of the surface and are probably H40.

3.4. DSC Measurements. DSC results show similar T_g for PPO film prepared in $CHCl_3$ and $CHCl_3$/NMP, respectively. Therefore, we compared the PPO−H40 to pure PPO in $CHCl_3$. Table 4 shows that the T_g of PPO−H40 1 wt % decreases to 209 °C in comparison with the pure PPO (T_g = 214 °C). The T_g of PPO−H40 9.1 wt % is however comparable with the pure PPO. Boltorn H40 has T_g at 42 °C and melting point at 63 °C. PPO−H40 1 wt % has one T_m at 241 °C, which is close to the T_m of pure PPO (251 °C). However, PPO−H40 9.1 wt % has two melting peaks at 215 °C and 239 °C probably corresponding to the two phases visualized by SEM. The presence of two distinct T_m confirms the phase separation at 9.1 wt % Boltorn.

3.5. Positron Annihilation Lifetime Spectroscopy (PALS). The free volume in PPO−H40 1 wt % and 9.1 wt % was determined by PALS and compared with the pure PPO sample. The PALS results of pure PPO prepared in $CHCl_3$ and those prepared in $CHCl_3$/NMP are very similar to each other; therefore, here we use for comparison only pure PPO in $CHCl_3$. Figure 8a shows the original lifetime spectra of the samples. In the evaluation of our results the term "dispersion" will be frequently used in the context of o-Ps lifetime. In older evaluation methods, the lifetime of o-Ps was accepted to reflect a mean hole size. Newer evaluation software, as the one used in this work, assumes a distribution of lifetimes. We believe this is more suitable assumption, as holes in a noncrystalline

Table 3. Elemental Composition of the H40 Pure, PPO Pure (in $CHCl_3$) and PPO−Boltorn Membranes Obtained by EDX

sample	C (wt %)	O (wt %)
H40 (powder)	75	25
H40 (pellet)	75	25
PPO pure (in $CHCl_3$)	96	4
PPO−H40 1.0 wt %	95	5
PPO−H40 9.1 wt %	93	7

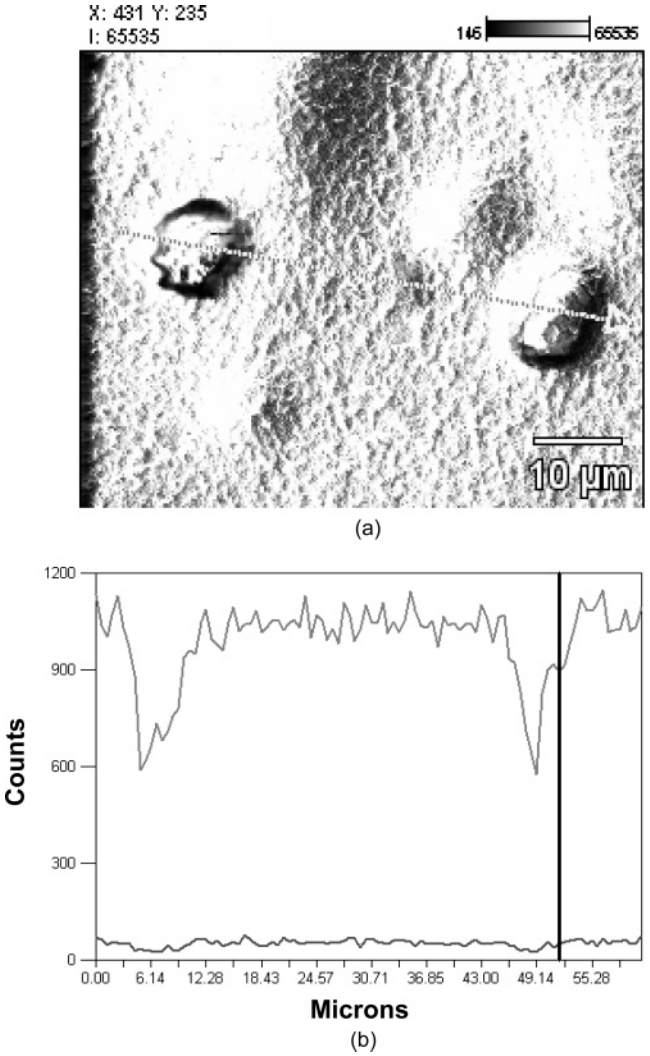

Figure 7. (a) SEM micrograph of PPO−H40 9.1 wt % membrane (top surface), (b) EDX spectra of PPO−H40 9.1 wt % membrane (accelerating voltage, 10.0 kV; magnification, 1000).

polymer are supposed to be distributed in size as well. This distribution is assumed to be log−normal, and the dispersion

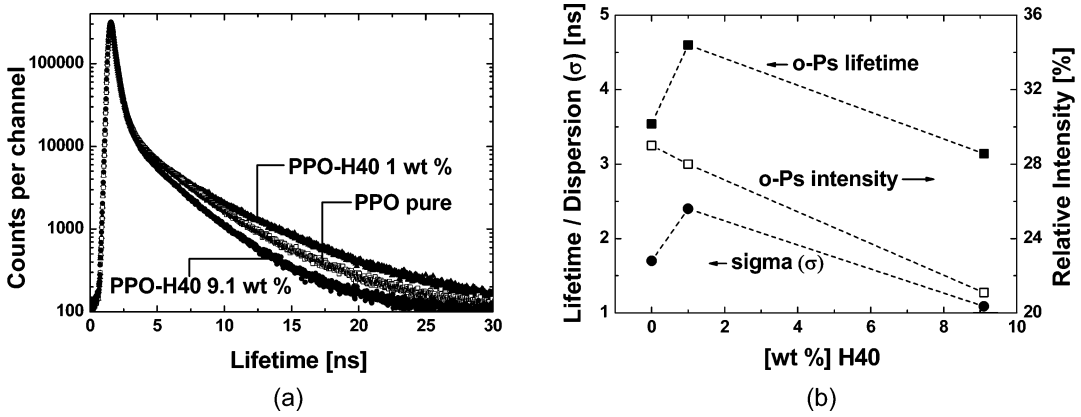

Figure 8. (a) PALS spectra of pure PPO (in $CHCl_3$) reference sample and PPO with different concentrations of Boltorn (1.0 and 9.1 wt %), (b) orthopositronium lifetime, dispersion (σ), and relative intensity, of pure PPO (in $CHCl_3$) and PPO−Boltorn.

Table 4. DSC Results of PPO, H40, and PPO−H40 Samples

samples	T_g (°C)	T_m (°C)
PPO	214	251
H40	42	63
PPO−H40 1.0 wt %	209	241
PPO−H40 9.1 wt %	212	215
		239

(or σ) given is the standard deviation of the log−normal lifetime distribution. The increase in orthopositronium lifetime reflects an increase of the average free volume size (indicator for average volume is the o-Ps lifetime, indicator for width is the dispersion, σ). The data are evaluated with respect to a single o-positronium lifetime, distribution and intensity (Figure 8b—the dotted lines are used to guide the eye and do not correspond to experimental data). The typical error in lifetime is ± 0.1 ns and about $\pm 1\%$ in intensity. This error includes the fitting error from the spectra and the reproducibility of the experiments under identical conditions. It was found[7] using PALS measurements that H40 has a free volume of 0.0635 nm^3. This will be taken into account in a more detailed data evaluation.

For the PPO−H40 1 wt % the o-Ps lifetime, as a measure of the average free volume and the dispersion is higher than pure PPO (see Figure 8b). The intensity decreases only slightly. This shows that the average free volume (increase of o-Ps lifetime) and the total free volume (increase of of o-Ps lifetime and σ) increases compared to the pure PPO. For the PPO−H40 9.1 wt %, o-Ps lifetime, dispersion and intensity decrease, indicating decreased free volume compared to pure PPO. At first glance, one would expect a further increase in free volume with increased concentration. However, if already 1 wt % of Boltorn increases the free volume and creates stress within the polymer structure, a further increase in concentration might shift the overall distribution of free volume to very high values. Therefore, it is possible that the largest holes are filled by Boltorn. Other holes, smaller than the critical size are contracted and also filled with Boltorn. Hence, the largest holes are filled, the larger part of the distribution of free volume is cut off, therefore average value and width of distribution decrease consequently the gas permeability decreases (see section 3.1). This hypothesis seems consistent with EDX measurement, which shows agglomerates of H40 for the PPO−H40 9.1 wt % membrane and the permeability measurements.

The PALS results suggest that the increased permeability of PPO containing low concentration of Boltorn (1.0 wt %) is due to increase of the average and total free volume of the PPO−H40 1.0 wt % sample in comparison to pure PPO. The interaction between the hydroxyl end groups of Boltorn with the electron pair of the oxygen atom of the PPO backbone may induce hydrogen bonds formation.[7,22] In such a way the 1.0 wt % of Boltorn molecules are retained in the PPO membrane phase by the hydrogen bonds introducing an extra interstitial chain space. This leads to an increased free volume and therefore to an increased permeability (Table 1). The decreased permeability of PPO containing higher concentration of Boltorn (9.1 wt %) is due to the decrease of polymer free volume. In this case the hyperbranched polyesters form aggregates (shown by EDX and SEM) in the large holes created, which can be stabilized by hydrogen bonding of terminal groups.[6] Two different models of crystallization can occur (proposed by Malmström[7]): intermolecular crystallization, without mixing of end groups and intramolecular crystallization. Most probably, during the drying process segregation of Boltorn occurs, preferentially at the air side of the film (as shown by SEM, section 3.2). Because the largest holes are filled, the larger part of the distribution of free volume is cut off and therefore the average and total free volume decreases leading to a decreased permeability, in agreement with the literature.[23]

3.6. WAXS Analysis. Figure 9a displays spectra of PPO powder (pw) and H40 powder (pw) as received, of PPO−H40 1.0 wt % and pure PPO (in $CHCl_3$/NMP) film. The results are displayed when the incident beam is perpendicular to the film (front view) and parallel to the film (side view), respectively. Main scattering peaks are numbered. Comparison of the scattering of pure PPO powder with pure PPO (in $CHCl_3$/NMP) (Figure 9a,b) clearly indicates strong similarity: peak positions and relative intensities are very similar.

The scattering of the PPO−H40 1.0 wt % is similar to pure PPO (Figure 9a, front view). The main difference in this spectrum is the enhancement of a low-intensity maximum in sample PPO−H40 (1.0 wt %)—peak 5—by the addition of a small amount of Boltorn to the PPO film. This peak seems also to be present in the PPO powder[24,25] although also with extreme low intensity. The same situation is also observed in the side view (Figure 9a) whereas the same peaks are slightly brighter. This is probably due to the anisotropy of the sample that favors the formation of crystal planes in the plane of the film.

Further increase of the Boltorn concentration to 9.1 wt %, leads to similar results (see Figure 9b, front and side view). The scattering intensities are stronger in the side view situation than in the front view. Furthermore, the strong and very broad pure Boltorn (H40) scattering peak placed almost at the same position of polymer peak number 2 ($2\theta \sim 16°$)

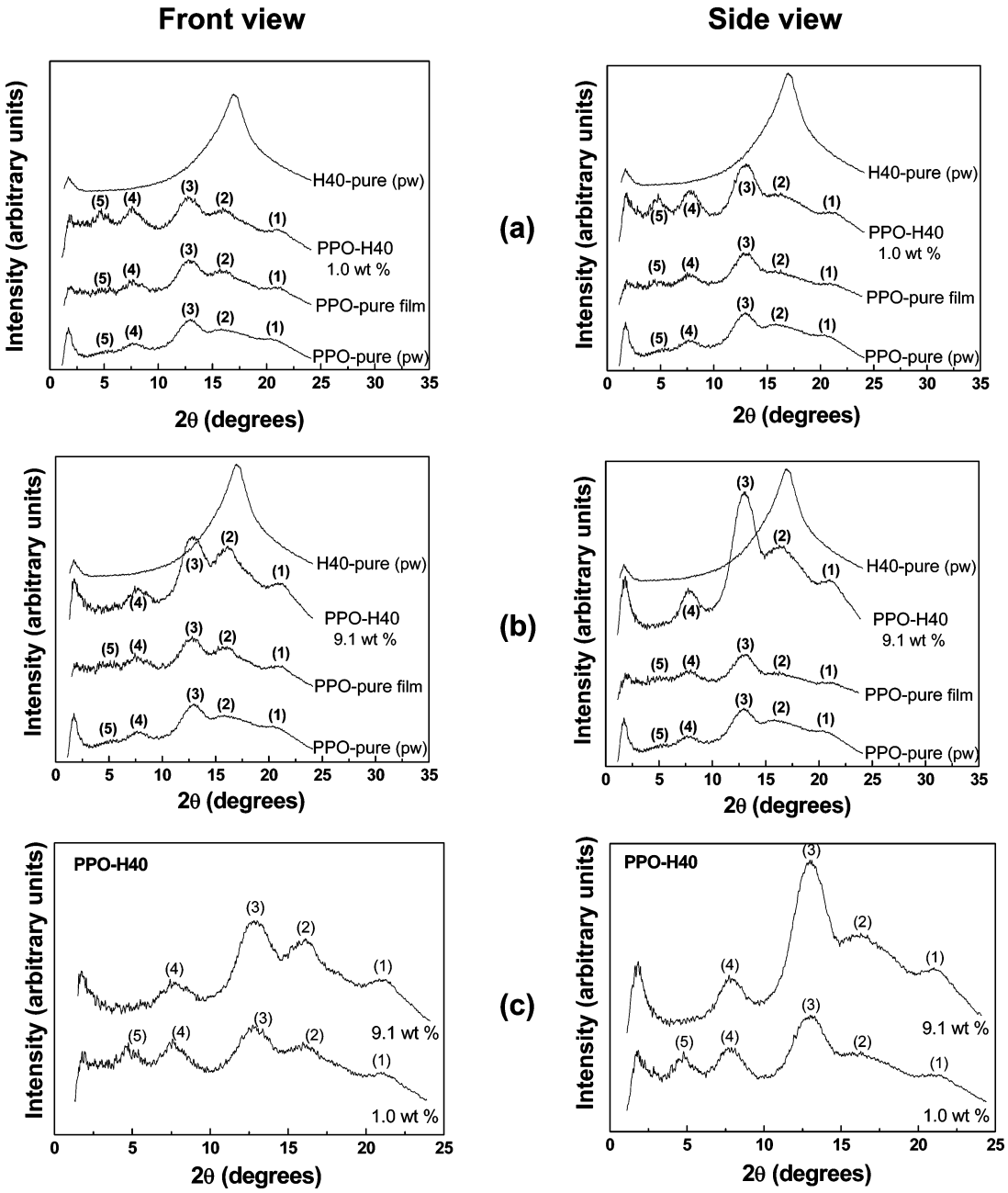

Figure 9. Scattering intensity as a function of the scattering angle of: (a) pure H40 powder, pure PPO powder, PPO−H40 1.0 wt % and pure PPO (in $CHCl_3$/NMP), (b) pure H40 powder, pure PPO powder, PPO−H40 9.1 wt % and pure PPO (in $CHCl_3$/NMP), (c) PPO−H40 1.0 wt % and 9.1 wt % H40. For part c, the scattering pattern of pure H40 multiplied by the volume fraction has been subtracted from PPO−H40.

strongly enhances most of the polymer peaks. Peak 5 ($2\theta \sim 5°$), is almost invisible in the PPO−H40 9.1 wt %, and this may be related to the fact that at that position, the contribution of the Boltorn scattering is the lowest in the whole scattering window. Peak number 5 appears as the less enhanced of the polymer peaks.

For better understanding of change in degree of crystallinity the scattering pattern of PPO−H40 1.0 wt % and PPO−H40 9.1 wt % H40 was plotted as a function of the scattering angle, where the scattering pattern of pure H40 multiplied by the volume fraction present in the sample has been subtracted from the films containing Boltorn (see Figure 9c). In this very qualitative analysis that also assumes that the Boltorn peak remains unchanged in the polymer matrix, it is very clear that enhancement of crystallinity occurs practically only in the plane of the film. Also, Figure 9a indicates the enhancement of peak 5 in the presence of low amounts of H40 while the other peaks seem to be enhanced with the increase of H40 amount (Figure 9b). Since the SEM micrographs show a phase separation in two rather distinct layers, it is reasonable to associate these WAXS results with this phenomenon.

Similar results are obtained for the scattering of mixtures of PPO and H20. Figure 10a displays results for PPO−H20 with incident beam perpendicular to the polymer film, and H20 concentrations of 1.0 and 9.1 wt %. A similar situation as for H40 is obtained and it is remarkable that the scattering curves are very similar, including the observations for peak 5 ($2\theta \sim 5°$) that become almost absent for higher Boltorn concentrations. Using the same arguments as above, these curves suggest that the presence of H20 does not introduce significant changes in PPO crystallinity in that direction in any of the studied concentrations. This is also the case for

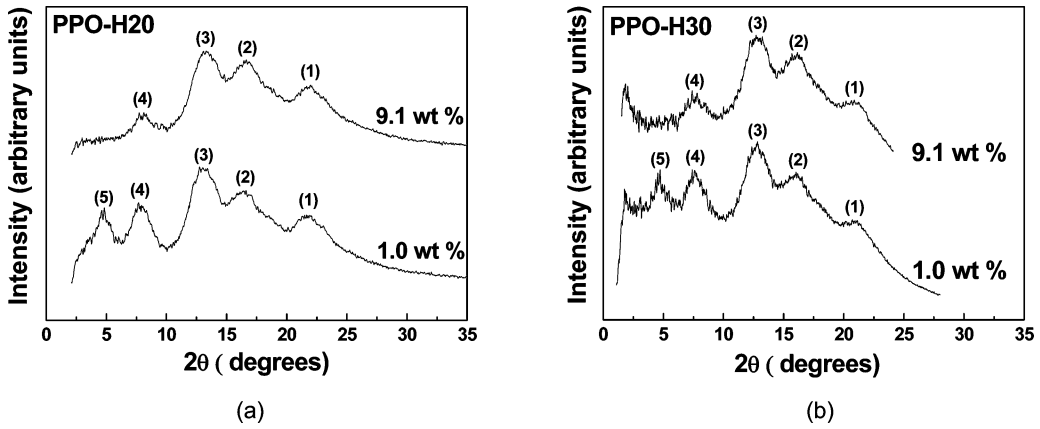

Figure 10. Scattering intensity (front view) as a function of the scattering angle: (a) PPO−H20 with 1.0 wt % and 9.1 wt % H20; (b) PPO−H30 with 1.0 wt % and 9.1 wt % H30.

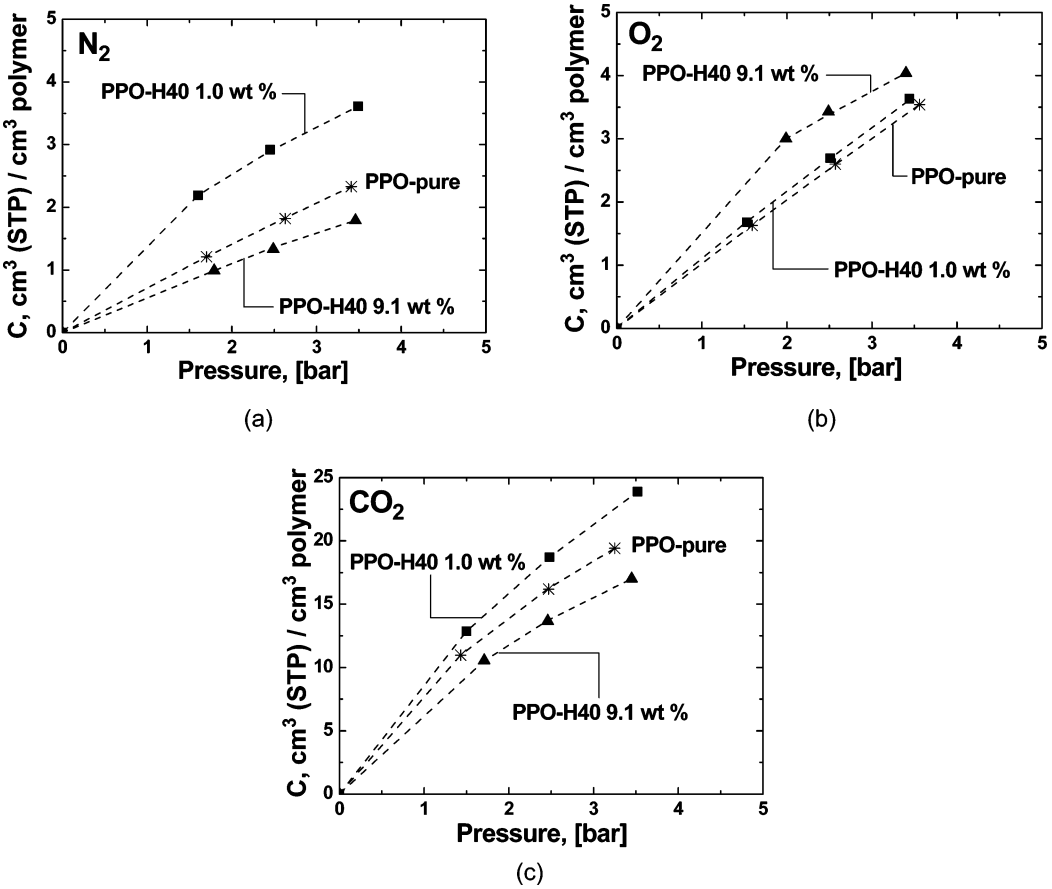

Figure 11. Sorption isotherms for (a) N_2, (b) O_2, and (c) CO_2 of PPO−H40 1.0 wt % H40 (■), and PPO−H40 with 9.1 wt % H40 (▲) in comparison to pure PPO (in $CHCl_3$/NMP) (∗). The dotted lines are model lines, which are fitted according to the dual mode sorption model. T = 35 °C.

PPO−H30 mixtures (Figure 10b) where scattering of samples containing 1.0 and 9.1 wt % are displayed. The curves are very similar as before. The "anomalous" scattering relating to peak 5 that is only present at lower Boltorn concentrations may have different origins. Nevertheless, it seems that it cannot be associated with the preparation conditions and solvent in the pure polymer film. The spectra of pure PPO (in $CHCl_3$/NMP) prepared with various NMP concentrations (Figure 9a,b) are extremely similar.

In conclusion, qualitatively, variation on the degree of crystallinity due to the presence of H40 is at maximum very small in the direction perpendicular to the film. It seems, however, enhanced in the direction of the film plane. The presence (or not) of the scattering peak 5 at 5° cannot be associated with the solvent composition used to prepare the films and its enhancement due to small amounts of Boltorn may be explained as follows. When small amounts of H40 are diluted in the PPO matrix, they produce inclusions of large curvature, while larger amounts aggregate, producing inclusions with much smaller curvature in the polymer matrix. Therefore, small amounts of H40 create higher stresses in the polymer matrix, leading to larger influence on the crystalline peaks of the matrix. In any case, a definitive explanation of this effect would require a more detailed systematic investigation, beyond the scope of the present work.

3.7. Gas Sorption. Figure 11 presents the sorption isotherms of CO_2, N_2, and O_2 through PPO−H40 1.0 wt %, and PPO−H40 9.1 wt % in comparison to pure PPO (in $CHCl_3$/NMP) at

Table 5. Gas Permeability, Solubility, and Diffusivity of PPO and PPO−H40 Films[a]

	N_2				O_2				CO_2			
membrane	*P*	*S*	D^b	D^c	*P*	*S*	D^b	D^c	*P*	*S*	D^b	D^c
PPO pure ($CHCl_3$)	2.7	8.4	3.2	3.1	11.7	11.0	10.7	9.9	50.7	78.3	6.5	5.3
PPO pure ($CHCl_3$/NMP)	4.4	9.5	4.6	4.1	16.2	13.7	11.8	11.9	63.9	101.0	6.3	5.9
PPO−H40 1.0 wt %	8.3	18.5	4.5	3.9	32.2	14.6	22.0	23.4	155.1	114.1	13.6	10.8
PPO pure ($CHCl_3$/NMP)	3.5	10.8	3.3	3.2	16.1	13.8	11.6	12.2	65.7	104.9	6.3	6.1
PPO−H40 9.1 wt %	2.0	7.4	2.7	2.4	7.6	22.2	3.4	3.8	38.1	84.8	4.5	4.9

[a] Feed pressure: 1.5 bar, $T = 35$ °C. P = [barrer], $S = 10^{-3}$, cm^3 (STP)/cm^3 cmHg, $D = 10^{-8}$, cm^2/s. [b] The diffusion coefficient D calculated from the P/S ratio. [c] The diffusion coefficient D calculated from the sorption kinetics.

35 °C. (The sorption isotherms for pure PPO prepared in various $CHCl_3$/NMP mixtures are similar.) The sorption isotherms are fitted by the dual mode sorption model.[26] For O_2 the difference in sorption between the PPO−H40 1.0 wt % and pure PPO is not significant. However, for PPO−H40 9.1 wt % the sorption is higher than the pure PPO. The segregated layer of H40 aggregates perhaps acts as an oxygen barrier material.[7] However, for N_2 and CO_2 the sorption is higher for PPO−H40 1.0 wt % due to the increase of free volume.

The sorption isotherms are necessary to deconvolute the permeability into its solubility and diffusivity contributions. Table 5 reports the permeability, solubility and diffusivity coefficients of N_2, O_2, and CO_2 gases of PPO−H40 1.0 wt %, PPO−H40 9.1 wt %, and PPO pure (in $CHCl_3$/NMP) at 35 °C and 1.5 bar feed pressure. Since some difference in gas permeability between the pure PPO prepared in $CHCl_3$ and $CHCl_3$/NMP, respectively were found (see Table 1) the results for pure PPO (in $CHCl_3$) are also presented. The solubility coefficient S was estimated from the gas sorption measurements and the diffusion coefficient D was calculated from the P/S ratio. To confirm the validity of this calculation, the diffusion coefficient D for all three gases was also calculated from the sorption kinetics using similar method as in literature.[12] The values of D found by both methods are generally in good agreement (see Table 5).

The N_2 diffusivity coefficients are about the same for PPO−H40 1.0 wt % and the PPO pure (in $CHCl_3$/NMP) membrane. Then, the increase of N_2 permeability for the PPO−H40 1.0 wt % membrane should be attributed to increase of S. For O_2 and CO_2 however, the increase of permeability through the PPO−H40 1.0 wt % in comparison to PPO pure can mostly be attributed to increase of D, while the solubility coefficients are rather comparable. This fits well with the results obtained by PALS (section 3.5) suggesting that the PPO−H40 1.0 wt % membrane has higher free volume. The free volume created in the polymer matrix is less accessible to fast diffusion of the big N_2 (with the highest gas molecule diameter from all three gases measured), although its solubility into membrane increases.

For the PPO−H40 9.1 wt % the decrease of N_2 and CO_2 permeability in comparison to pure PPO seems to be due to the decrease of both S and D. For O_2 the decrease of permeability could be attributed to decrease of D. The decrease of diffusion coefficient D can be a result of phase separation (Boltorn clustering) leading to a lower free volume (as seen by PALS, section 3.5). Interestingly, the solubility of O_2 to the PPO−H40 9.1 wt % dispersed membranes increases in comparison to pure PPO, probably due to an increase O_2 affinity induced by the higher Boltorn content.

3.8. Conclusions. The gas permeability of PPO−Boltorn 1.0 wt % increases more than two times than the pure polymer (prepared in the same solvent mixture), while at higher concentration of Boltorn (9.1 wt %) the permeability becomes lower than pure PPO. The increase in permeability at low concentration of Boltorn in PPO is due to increase of the polymer free volume. The interaction between the hydroxyl end groups of Boltorn with the electron pair of the oxygen atom of the PPO backbone may induce hydrogen bonds formation creating a more open structure.

The decreased permeability of PPO containing higher concentration of Boltorn (9.1 wt %) is due to the Boltorn aggregation, and reduced free volume. Because of a large number of peripheral hydroxyl groups the Boltorn may have stronger intermolecular interaction. Therefore, at higher Boltorn concentrations in PPO, they form aggregates that migrate to the membrane surface. This phenomenon leads to phase separation and loss of the free volume and therefore to a decrease in gas permeability.

Acknowledgment. This work was financially supported by The Netherlands Organization for Scientific research (STW−NWO, Project TPC.5776). The authors wish to thank Dr. Mircea Manea for the support and Boltorn supply and Dr. Arie Zwijnenburg for the EDX measurements.

References and Notes

(1) Wang, Y.-C.; Huang, S.-H.; Hu, C.-C.; Li, C.-L.; Lee, K.-R.; Liaw, D.-J.; Lai, J.-Y. *J. Membr. Sci.* **2004**, *248*, 15−25.
(2) Freeman, B. D. *Macromolecules* **1999**, *32*, 375.
(3) Albers, J. H. M.; Smid, J.; Kusters, A. P. M. "Gas separation apparatus and also method for separating gases by means of such an apparatus", US Patent 5,129,920, 1992.
(4) Mulkern, T. J.; Beck, Tan, N. C. *Polymer* **2000**, *41*, 3193−3203.
(5) Hsieh, T.-T.; Tiu, C.; Simon, G. P. *Polymer* **2001**, *42*, 1931−1939.
(6) Rogunova, M.; Lynch, T.-Y. S.; Pretzer, W.; Kulzick, M.; Hiltner, A.; Baer, E. *J. Appl. Polym. Sci.* **2000**, *77*, 1207−1217.
(7) Rittinge, R. Free Volume Characterization of Hyperbranched Polymers, Bachelor thesis, Lund University, Sweden, 2002.
(8) Pettersson, B. *Properties and Applications of Dendritic polymers*; Sweden, 2001.
(9) Barsema, J. N.; Kapantaidakis, G. C.; van der Vegt, N. F. A.; Koops, G. H.; Wessling, M. *J. Membr. Sci.* **2003**, *216*, 195.
(10) Visser, T.; Koops, G. H.; Wessling, M. *J. Membr. Sci.* **2005**, *252*, 265−277.
(11) Crank, J. *The mathematics of diffusion*, 2nd ed.; Clarendon Press: Oxford, U.K., 1975.
(12) Visser, T. Mixed gas plasticization phenomena in asymmetric membranes. Ph.D. thesis, 2006.
(13) Sterescu, D. M.; Stamatialis, D. F.; Mendes, E.; Wübbenhorst, M.; Wessling, M. *Macromolecules* **2006**, *39*, 9234−9242.
(14) Kruse, J.; Kanzow, J.; Rätzke, K.; Faupel, F.; Heuchel, M.; Frahn, J.; Hofmann, D. *Membr. News* **2004**, *66*, 51−54.
(15) Kruse, J.; Kanzow, J.; Rätzke, K.; Faupel, F.; Heuchel, M.; Frahn, J.; Hofmann, D. *Macromolecules* **2005**, *38*, 9638−9643.
(16) Eldrup, M.; Lightbody, D.; Sherwood, J. N. *J. Chem. Phys.* **1981**, *63*, 51.
(17) Tao, S. J. *J. Chem. Phys.* **1972**, *56*, 5499.
(18) Nagel, C.; Schmidtke, E.; Günther-Schade, K.; Hofmann, D.; Fritsch, D.; Strunskus, T.; Faupel, F. *Macromolecules* **2000**, *33*, 2242−2248.
(19) Jean, Y. C. *Principles and applications of positron & positronium chemistry*, World Scientific: Singapore, 2003.
(20) Xiao, Y.; Chung, T.-S.; Chng, M. L. *Langmuir* **2004**, *20*, 8230−8238.
(21) Boogh, L.; Pettersson, B.; Månson, J.-A. E. *Polymer* **1999**, *40*, 2249−2261.
(22) Polotskaya, G. A.; Gladchenko, S. V.; Pen'kova, A. V.; Kuznetsov, V. M.; Toikka, A. M. *Russ. J. Appl. Chem.* **2005**, *78*, 1468−1473.

(23) Aoki, T.; Kaneko, T. *Polym. J.* **2005**, *37*, 717.

(24) Chowdhury, G.; Kruczek, B.; Matsuura, T. *Polyphenylene Oxide and Modified Polyphenylene Oxide Membranes Gas, Vapor and Liquid Separation*; Kluwer Academic Publishers: New York, 2001.

(25) Khulbe, K. C.; Matsuura, T.; Lamarche, G.; Lamarche, A.-M. *J. Membr. Sci.* **2000**, *170*, 81−89.

(26) Kanehashi, S.; Nagai, K. *J. Membr. Sci.* **2005**, *253* (*1*−*2*), 117−138.

MA070772G